

# Chapter 23

## 2D Methods for the Measurement of Long-Range Proton–Carbon Coupling Constants

Teodor Parella

*Servei de Resonància Magnètica Nuclear, Universitat Autònoma de Barcelona, E-08193, Bellaterra, Barcelona, Spain*

23.1 Introduction	305
23.2 $^{13}\text{C}$ -Detected NMR Methods	306
23.3 $^1\text{H}$ -Detected NMR Methods	307
23.4 Miscellaneous NMR Methods	311
23.5 Summary	312
References	313

### 23.1 INTRODUCTION

Heteronuclear long-range proton–carbon coupling constants ( $^nJ_{\text{CH}}$ ;  $n > 1$ ) are important parameters in the structural, stereochemical, and conformational analysis of small- and medium-sized organic compounds at natural abundance. In particular, J-configuration analysis has been proposed to study stereochemical and conformational properties of both rigid and flexible organic molecules and natural products by concerted use of homonuclear proton–proton ( $J_{\text{HH}}$ ) and heteronuclear  $^nJ_{\text{CH}}$  coupling constants as well as homonuclear  $^1\text{H}$ – $^1\text{H}$  NOEs.<sup>1</sup> The magnitudes of such  $^nJ_{\text{CH}}$  interactions rarely exceed 10–12 Hz. It is generally assumed that

two-bond coupling constants ( $^2J_{\text{CH}}$ ) are small in magnitude and of negative sign; they can sometimes be experimentally correlated with substitution patterns and bond orientations in  $^1\text{H}$ – $\text{C}$ – $^{13}\text{C}$ – $\text{X}$  spin systems. On the other hand, three-bond coupling constants ( $^3J_{\text{CH}}$ ) typically have positive sign and they can be correlated with dihedral angles in  $^1\text{H}$ – $\text{C}$ – $\text{C}$ – $^{13}\text{C}$  spin systems following classical Karplus-type relationships.<sup>2,3</sup> Correlations that are of longer range than three-bond become uninformative because their values are usually  $< 1$  Hz.

In contrast to the obvious interest of  $^nJ_{\text{CH}}$  coupling constants, their practical use has been severely hampered by the difficulty of their precise quantitative measurement. Many different NMR approaches have been proposed during recent decades, but no general method exists for this purpose. A good method should have optimum sensitivity, the extraction of the J magnitude must be simple and precise, the determination of the sign can be of interest, and it must be of general applicability to a wide range of products and conditions. Sometimes, the concerted application of different but complementary NMR techniques is performed to avoid the limitations of each individual method. The purpose of this article is to provide a short overview of modern NMR methods

to measure  $^nJ_{\text{CH}}$  coupling constants. Readers interested in a more complete and detailed description are directed to the excellent and comprehensive review published by Márquez *et al.*<sup>4</sup> or to the original references.

## 23.2 $^{13}\text{C}$ -DETECTED NMR METHODS

The first proposed NMR methods to measure  $^nJ_{\text{CH}}$  were based on  $^{13}\text{C}$ -detection, and therefore, they all show an important sensitivity penalty when compared to modern proton-detected experiments. The simplest approach is to record a fully or partially  $^1\text{H}$ -coupled 1D  $^{13}\text{C}$  spectrum; this can be extended to analogous  $^1\text{H}$ -coupled INEPT-based

and DEPT-based experiments. The main limitation arises from complex, poorly resolved multiplets, and successful application is often limited to relatively simple spin systems. In addition Bloch–Siegert effect multiplet distortions (where selective proton decoupling is used) and low resolution can introduce important errors.

With the advent of multipulse heteronuclear 2D sequences,  $^nJ_{\text{CH}}$  values were determined approximately by cross-peak intensity analysis or more accurately by direct measurement of multiplet splittings in modified long-range optimized HETCOR or COLOC experiments (see a complete description of these NMR experiments in Chapter 22). However, the most interesting applications were based on heteronuclear J-resolved pulse schemes (see also Chapter 11). Bax and Freeman proposed a very

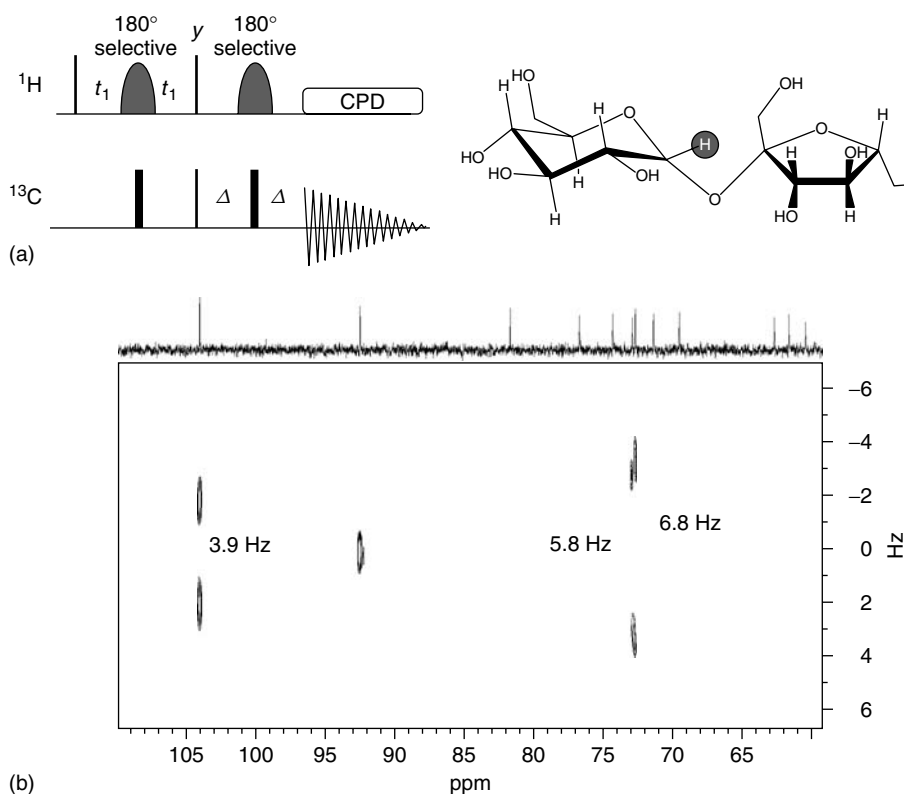


**Figure 23.1.** (a) 2D  $^1\text{H}$ -selective carbon-detected J-resolved INEPT pulse scheme. Selective  $^1\text{H}$   $180^\circ$  pulses are applied to a chosen well-isolated proton resonance and the interpulse delay  $\Delta$  is optimized to  $1/(4^n J_{\text{CH}})$ . (b) 2D selective J-INEPT spectrum with inversion of the glucose H-1 proton of sucrose in  $\text{D}_2\text{O}$  (see chemical structure). The active coupling constants are well resolved as doublet signals in the indirect dimension.

simple proton-selective 2D-J-resolved experiment that yields the magnitude of  ${}^nJ_{\text{CH}}$  with good resolution from the splitting generated in the indirect dimension.<sup>5</sup> The main limitations of this method are the low sensitivity associated with  ${}^{13}\text{C}$  detection, and the need for a well-isolated proton resonance to be selectively inverted. Some related applications were developed using sensitivity-improved polarization transfer schemes, such as the selective 2D INEPT-J experiment shown in Figure 23.1(a).<sup>6</sup> This experiment is based on a long-range optimized refocused INEPT pulse train, and the resulting 2D  ${}^{13}\text{C}$  spectrum presents a very simple pattern, showing only the carbon resonances correlating with

the selected proton and showing the  ${}^nJ_{\text{CH}}$  coupling value as a clean doublet in the indirect dimension (Figure 23.1b).

### 23.3 ${}^1\text{H}$ -DETECTED NMR METHODS

The design of highly sensitive proton-detected NMR methods enhanced with gradient coherence selection afforded new and improved approaches to measure heteronuclear coupling constants (see also Chapter 22). In practice, the most challenging task is to observe the tiny signal due to the  ${}^1\text{H}\text{--}\text{X}\text{--}{}^{13}\text{C}$  or  ${}^1\text{H}\text{--}\text{X}\text{--}\text{Y}\text{--}{}^{13}\text{C}$  isotopomers (1.1% at natural

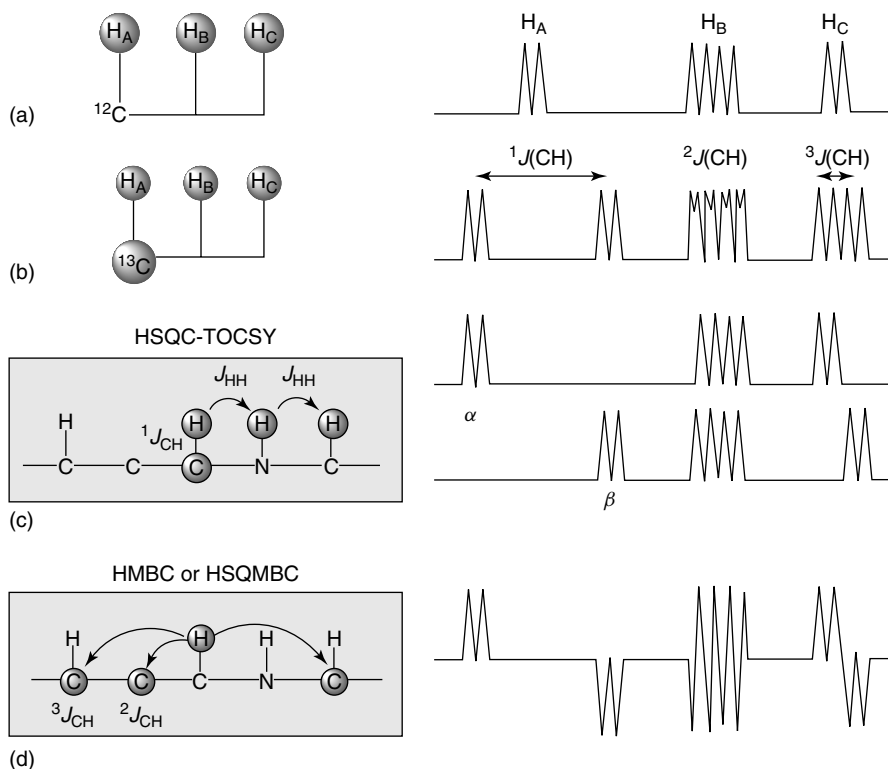


**Figure 23.2.** Typical  ${}^1\text{H}$  NMR spectra of hypothetical (a)  ${}^1\text{H}({}^{12}\text{C})\text{--}{}^1\text{H}(\text{X})\text{--}{}^1\text{H}(\text{Y})$  and (b)  ${}^1\text{H}({}^{13}\text{C})\text{--}{}^1\text{H}(\text{X})\text{--}{}^1\text{H}(\text{Y})$  spin systems. In (b) each resonance shows an additional splitting due to the  $J$  coupling with the active  ${}^{13}\text{C}$  nucleus. Although  $J_{\text{CH}}$  coupling constants could sometimes be measured from (b), it is more advisable to obtain two separate spin-edited spectra, as shown in (c). The direct analysis of the relative displacement between signals affords the sign and the magnitude, even for very small coupling values. This approach is usually performed in HSQC-TOCSY experiments that use a sequential, two-step ( ${}^1J_{\text{CH}} + {}^1J_{\text{HH}}$ ) transfer mechanism. (d) Long-range correlation experiments, such as HMBC or HSQMBC, afford antiphase coupling patterns with respect to  ${}^nJ_{\text{CH}}$ . Additionally,  $J_{\text{HH}}$  modulation can take place during evolution delays, making it difficult to get precise  $J$ -coupling measurement because of multiplet distortions. A fitting procedure using reference multiplets (such as shown in (a)) may be required.

abundance) in the presence of their enormous  $^{12}\text{C}$  counterparts in the conventional  $^1\text{H}$  NMR spectrum. Figure 23.2 shows theoretical  $^1\text{H}$  NMR spectra for  $^{12}\text{C}$  and  $^{13}\text{C}$  isotopomers (Figure 23.2a and b, respectively) and some different approaches proposed for measuring  $^nJ_{\text{CH}}$  in  $^{13}\text{C}$ -active molecules. Robust pulse sequences are needed to efficiently remove the large  $^{12}\text{C}$  resonances, while giving clean and well-resolved cross peaks for  $^{13}\text{C}$  resonances. Basically, two different approaches are now available: (i) methods employing the fundamentals of the HSQC-TOCSY experiment, which involve a sequential two-step in-phase magnetization transfer ( $^1J_{\text{CH}} + J_{\text{HH}}$ ) for the measurement of  $^nJ_{\text{CH}}$  on protonated carbons but fail for quaternary carbons or for inefficient HH TOCSY transfer; and (ii) NMR experiments based on long-range optimized heteronuclear correlations, such as HMBC or long-range HSQC (HSQMBC) experiments, which can be used for both protonated and nonprotonated carbons. The latter experiments present antiphase coupling patterns (Figure 23.2d) and more complex data analysis is required.

Other miscellaneous proton-detected experiments have also been reported, as briefly described in 23.4.

### 23.3.1 HSQC-TOCSY-Type Experiments

A number of different approaches are available for extracting the magnitudes of J-coupling constants from multiplet patterns in multidimensional NMR spectra (Figure 23.3). The in-phase nature of TOCSY-like multiplet patterns (Figure 23.2b) is usually coded into two separate contributions (Figure 23.2c) using the concept of spin-state selection, such as in-phase/antiphase (IPAP) or E.COSY (see also Chapter 14), from which the measurement of both the sign and the magnitude of  $^nJ_{\text{CH}}$  is easy and effective.

The first proton-detected experiment proposed was a  $F_1$ - $^{13}\text{C}$ -filtered TOCSY pulse sequence, referred to as *HETLOC*,<sup>7,8</sup> that affords a  $^1\text{H}$ - $^1\text{H}$  correlation map with E.COSY-type multiplet patterns. The main limitations of this technique are the low dispersion

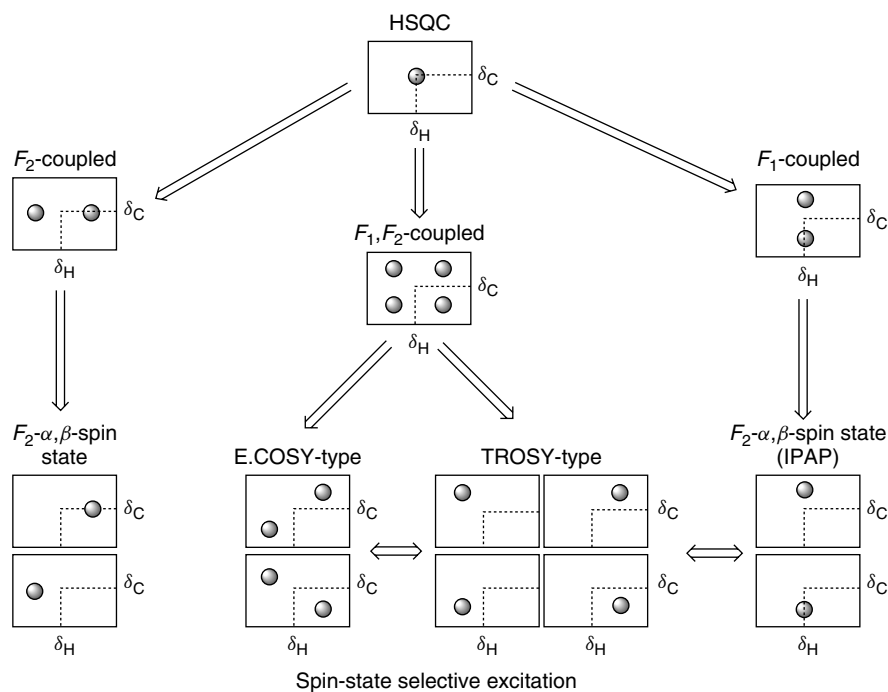


**Figure 23.3.** Coupling patterns produced by different classes of 2D NMR spectra. Spin-state selection methods afford a powerful way to split multiplet components into different NMR spectra, allowing easy and precise measurement even of small  $J$  values and avoiding signal overlap.

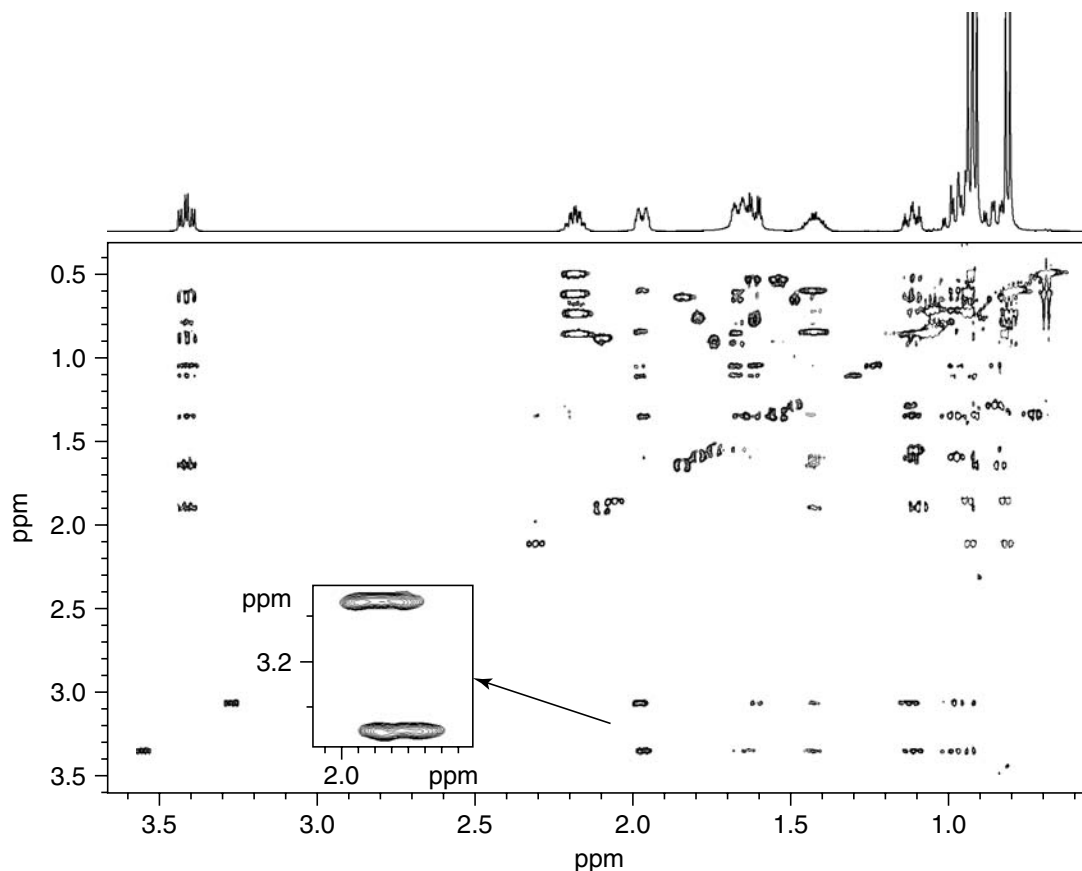


**Figure 23.4.** 2D HETLOC spectrum of menthol. The signs and magnitudes of  $^nJ_{\text{CH}}$  coupling constants are extracted directly by analyzing the relative E.COSY displacement of the two cross-peak components, as shown in the inset.

in the indirect  $^1\text{H}$  dimension and, very importantly, that each  $^1\text{H}$  resonance generates two cross peaks (Figure 23.4), increasing the number of peaks in the final spectrum and therefore also increasing the possibility of signal overlap. HETLOC has been widely used, but signal overlap can be a serious limitation in congested spectral regions.

In general, it is more advantageous to perform HSQC-type experiments because of the much better dispersion in the indirect  $^{13}\text{C}$  dimension. The simplest experiment is the measurement of  $^nJ_{\text{CH}}$  from the additional splitting generated in the direct  $F_2$  dimension of a conventional HSQC-TOCSY experiment performed without decoupling during acquisition.<sup>9</sup> A comparison with a reference uncoupled cross peak allows the extraction of the  $J$  value, although this can be difficult in complex multiplets.

Improved approaches introduce the IPAP<sup>9,10</sup> or E.COSY<sup>11,12</sup> techniques mentioned above that afford different types of multiplet patterns. For instance, the 2D HSQC-TOCSY-IPAP pulse scheme shown in Figure 23.5(a) is a straightforward modification of the sensitivity-enhanced HSQC experiment,<sup>13</sup> with a TOCSY transfer inserted into the PEP block and with the omission of X-decoupling during  $^1\text{H}$  acquisition; it affords clean spin-state selection for all three multiplicities  $\text{CH}$ ,  $\text{CH}_2$ , and  $\text{CH}_3$ . Two different datasets are recorded, HSQC-IP (with  $\phi_2 = y$  and  $\phi_3 = x$ ) and HSQC-AP (with  $\phi_2 = x$  and  $\phi_3 = y$ ). Figure 23.5(b) shows the edited spectra after coaddition and cosubtraction of the IP and AP data, respectively. The number of peaks in each edited spectrum is the same as in the regular HSQC-TOCSY experiment, reducing the probability

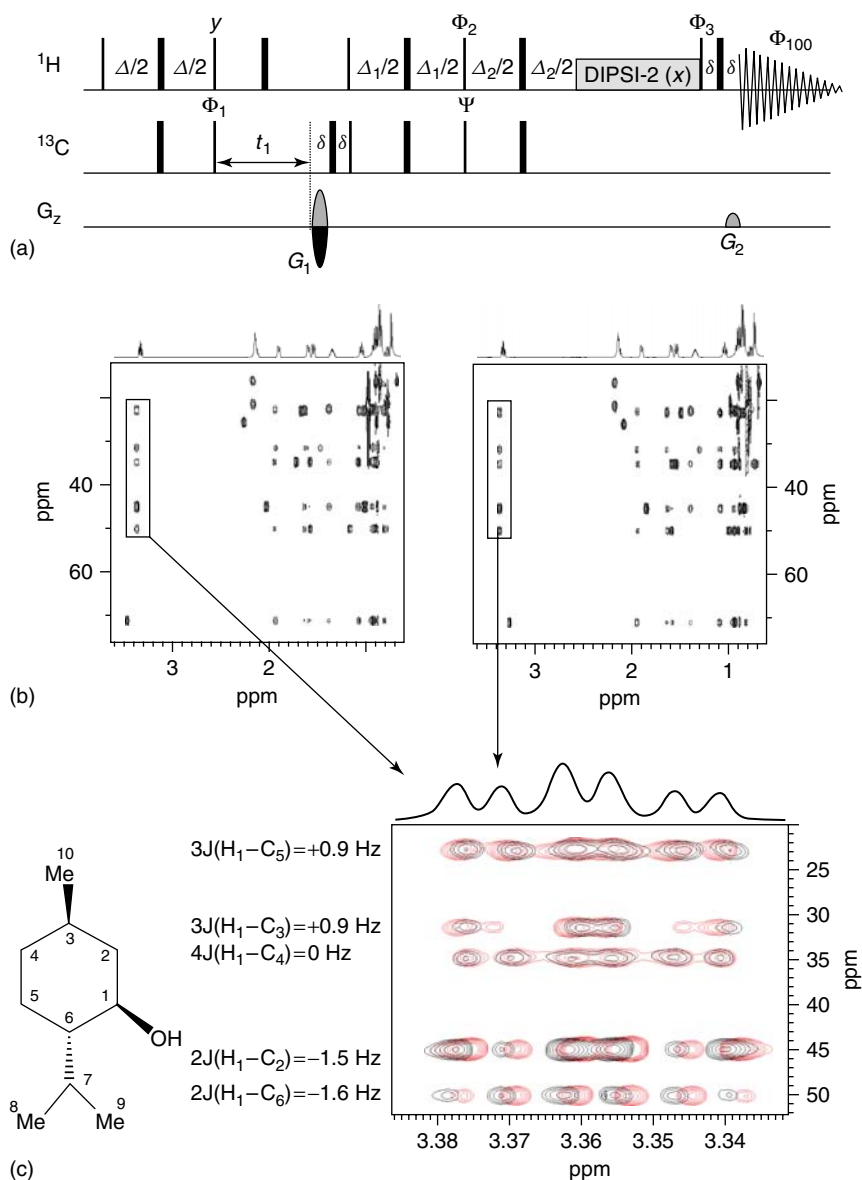


**Figure 23.5.** (a) Pulse scheme of the sensitivity-enhanced 2D HSQC-TOCSY experiment for the measurement of  $^nJ_{\text{CH}}$  coupling constants. Two different datasets are recorded separately as a function of  $\phi_2$  and  $\phi_3$ , and appropriate linear combinations afford the separate  $\alpha/\beta$  spectra as shown in (b) (see text for details). (c) Expansion plot for the  $\text{H}_1$  proton of menthol in the spectrum of Figure 23.2(b). The two spectra are overlapped to visualize. The sign and the magnitude are extracted directly by analyzing the relative displacements of cross peaks in the two overlapped spectra.

of signal overlap. Direct analysis of the relative displacement of each edited cross peak affords the sign and the magnitude of  $^nJ_{\text{CH}}$ , as shown in Figure 23.5(c). Additional features of this experiment

are as follows: coupling constants smaller than the line width can be measured with high accuracy, it can be useful for chemical assignment purposes, and the signs of coupling constants can be used

for a tentative distinction between two-bond and three-bond connectivities.

### 23.3.2 Long-Range $^1\text{H}$ – $^{13}\text{C}$ Correlation Experiments

Long-range J(CH) optimized pulse sequences based on the original HMQC or HSQC pulse trains can be used for the measurement of  $^nJ_{\text{CH}}$  on both protonated and nonprotonated carbon centers. However, in contrast to HSQC-TOCSY-type experiments, the success of these experiments depends of the efficiency of the single long-range CH transfer and, therefore, it is usually complicated to use them to measure small  $^nJ_{\text{CH}}$  values. Thus, a series of modified HMBC-like<sup>14</sup> and HSQMBC-like<sup>15</sup> experiments (Figure 23.6a) have been proposed to measure these, focusing on the measurement of quaternary carbons where the above-mentioned HSQC-TOCSY-like experiments cannot be applied. A major inconvenience is that these experiments afford antiphase multiplet patterns that cause partial signal cancellation and peak-maximum displacement, which are serious problems for precise  $^nJ_{\text{CH}}$  measurement (Figure 23.6). In addition to requiring good spectral resolution in the detected dimension, a postprocessing fitting procedure is usually mandatory, using additional data from reference signals.

Because the experimental signal intensity for a given cross peak directly depends on the  $^nJ_{\text{CH}} \cdot \text{delay}$  product, the measurement of small  $^nJ_{\text{CH}}$  values is usually a challenging task. Improved HSQMBC experiments introducing CPMG-like CH transfers have been proposed to minimize undesired  $J_{\text{HH}}$  phase modulation that complicates signal analysis.<sup>16</sup>

## 23.4 MISCELLANEOUS NMR METHODS

A number of 1D carbon-selective analogs of the proton-detected 2D HMBC, HSQMBC, and HSQC-TOCSY experiments described previously have been proposed for determining  $^nJ_{\text{CH}}$ .<sup>17</sup> The main advantages are better resolution and faster acquisition of individual 1D spectra when compared to the corresponding 2D analogs, and the only added experimental requirement is the successful application of a carbon-selective pulse. On the other

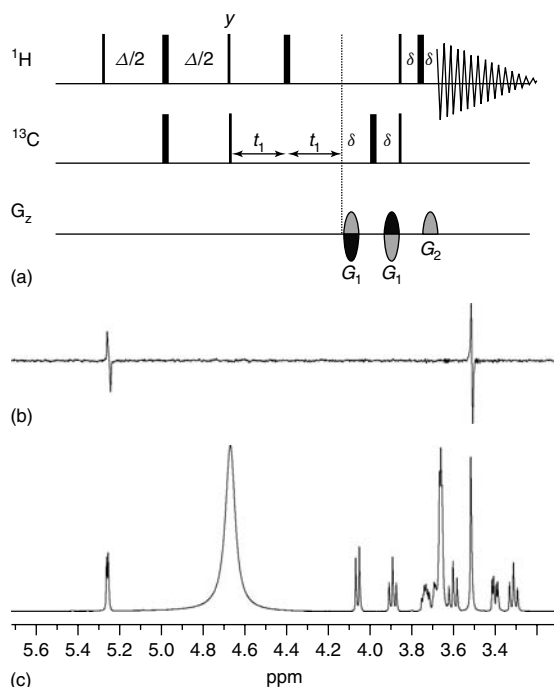


**Figure 23.6.** (a) Pulse scheme for a 2D long-range optimized HSQC (HSQMBC) experiment to measure  $^nJ_{\text{CH}}$ . (b) 1-D slice taken in the direct dimension for the quaternary carbon of sucrose, showing two antiphase cross peaks. Comparison with reference multiplets extracted from the conventional  $^1\text{H}$  NMR spectrum (c) allows  $^nJ_{\text{CH}}$  to be extracted. Sometimes a fitting procedure is required, as described in Reference 14.

hand, 3D versions of the HSQC-TOCSY experiments have also been proposed to avoid accidental signal overlap in overcrowded 2D spectra.<sup>18</sup> Analogous 1D and 2D experiments based on selective heteronuclear cross polarization have also been proposed.<sup>19,20</sup>

The concept of J-modulation during the indirect dimension of the heteronuclear correlation experiment has been also implemented in J-resolved HMBC experiments.<sup>21–24</sup> In these spectra, long-range correlation peaks appear as doublet splittings in the indirect  $F_1$  dimension. The lack of resolution in the indirect dimension and undesired  $J_{\text{HH}}$  modulation can be overcome by using constant-time versions of the experiments, and by introducing a scaling factor  $k$  that amplifies the  $J$  value to  $k \cdot J_{\text{CH}}$  (Figure 23.7). Proton-detected carbon-selective versions of the heteronuclear J-resolved experiment have

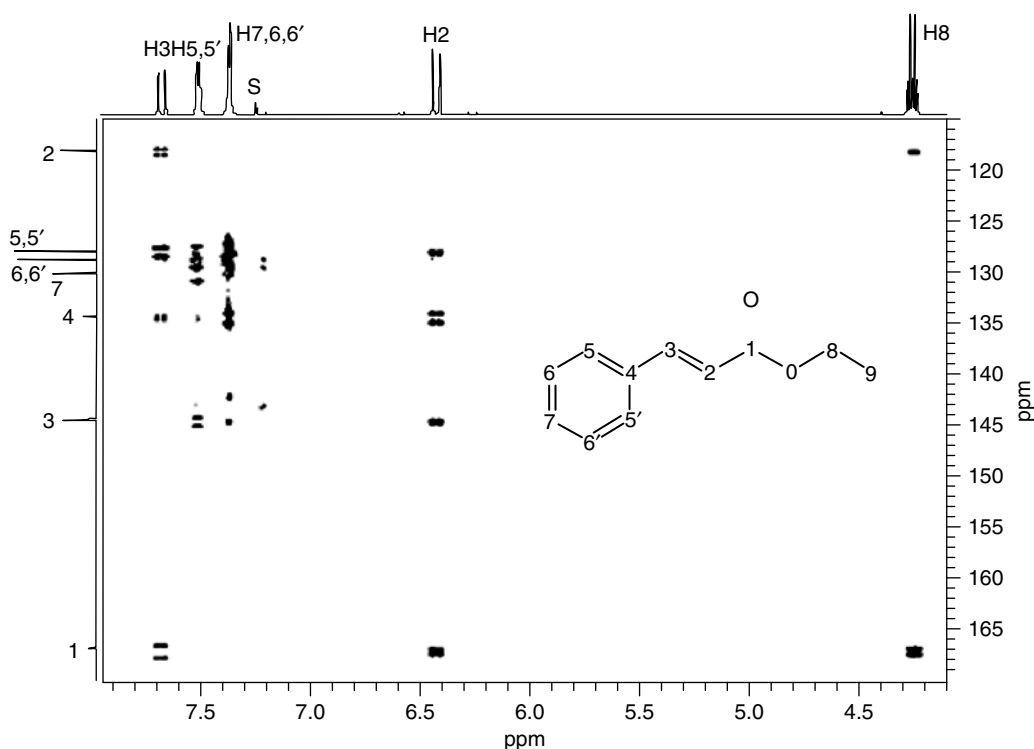


**Figure 23.7.** 2D constant-time J-HMBC spectrum of ethyl *trans*-cinnamate using a scaling factor  $k = 22$ . Note that all cross peaks appear with an apparent splitting of the doublet components by a factor  $k \cdot J_{\text{CH}}$  in the indirect dimension. (Reproduced from Ref. 22. © John Wiley & Sons Ltd., 2001.)

also been proposed, offering excellent resolution in the  $F_1$  dimension.<sup>25</sup>

Several NMR methods have also been proposed for correlating the intensities of cross peaks with  $^nJ_{\text{CH}}$  magnitudes in HMBC experiments.<sup>26,27</sup> They only provide a low accuracy estimate of the  $^nJ_{\text{CH}}$  value, and a second, reference, spectrum is usually required. The principles described here can be applied to measure coupling constants with other heteronuclei, for instance,  $^{31}\text{P}$  or  $^{15}\text{N}$ . Thus, it has been proposed to measure  $^nJ_{\text{CH}}$  and  $^nJ_{\text{NH}}$  (proton–nitrogen coupling constants) simultaneously in a single time-shared HSQC-TOCSY or HSQMBC experiment.<sup>28</sup>

### 23.5 SUMMARY

A great number of different NMR methods have been proposed during the last three decades for measuring  $^nJ_{\text{CH}}$  at natural abundance. However, nowadays,

two general approaches are used. For protonated carbons, the sensitive HSQC-TOCSY experiment is the method of choice because it provides both the magnitude and the sign of  $^nJ_{\text{CH}}$ , by analyzing the relative displacement between edited cross peaks without any postprocessing fitting procedure. The method can measure  $J$  values smaller than the line width with excellent accuracy, and the intensities of cross peaks basically depend on the efficiency of the  $J_{\text{HH}}$  TOCSY transfer. For nonprotonated carbons, phase-sensitive versions of long-range HMBC or HSQMBC correlation experiments are the methods of choice. Antiphase coupling patterns are generated, and a fitting procedure is, therefore, required for an accurate measurement. The sensitivity of the experiment depends directly on the long-range  $J_{\text{CH}}$  transfer, and therefore, the measurement of small coupling values on nonprotonated carbons is usually challenging. Alternatively, J-resolved and selective NMR methods can also be of interest in particular cases.



## RELATED ARTICLES IN THE ENCYCLOPEDIA OF MAGNETIC RESONANCE

### Heteronuclear Assignment Techniques

### Indirect Coupling: Theory and Applications in Organic Chemistry

### INEPT

### Polarization Transfer Experiments via Scalar Coupling in Liquids

### Stereochemistry and Long Range Coupling Constants

### Vicinal Coupling Constants and Conformation of Biomolecules

## REFERENCES

1. R. Riccio, G. Bifulco, P. Cimino, C. Bassarello, and L. Gomez-Paloma, *Pure Appl. Chem.*, 2003, **75**, 295.
2. R. Aydin and H. Günther, *Magn. Reson. Chem.*, 1990, **28**, 448.
3. R. H. Contreras and J. E. Peralta, *Prog. Nucl. Magn. Reson. Spectrosc.*, 2000, **37**, 321.
4. B. L. Márquez, W. H. Gerwick, and R. T. Williamson, *Magn. Reson. Chem.*, 2001, **39**, 499.
5. A. Bax and R. Freeman, *J. Am. Chem. Soc.*, 1982, **104**, 1099.
6. M. Hricovíni and T. Liptaj, *Magn. Reson. Chem.*, 1989, **27**, 1052.
7. M. Kurz, P. Schmieder, and H. Kessler, *Angew. Chem. Intl. Ed.*, 1991, **30**, 1329.
8. D. Uhrín, G. Batta, V. J. Hruby, P. N. Barlow, and K. E. Kövér, *J. Magn. Reson.*, 1998, **130**, 155.
9. W. Kozminski, *J. Magn. Reson.*, 1999, **137**, 408.
10. P. Nolis, J. F. Espinosa, and T. Parella, *J. Magn. Reson.*, 2006, **180**, 39.
11. W. Kozminski and D. Nanz, *J. Magn. Reson.*, 1997, **124**, 383.
12. P. Nolis and T. Parella, *J. Magn. Reson.*, 2005, **176**, 15.
13. L. E. Kay, P. Keifer, and T. Saarinen, *J. Am. Chem. Soc.*, 1992, **114**, 10663.
14. R. A. E. Edden and J. Keeler, *J. Magn. Reson.*, 2004, **166**, 53.
15. R. T. Williamson, B. L. Márquez, W. H. Gerwick, and K. E. Kövér, *Magn. Reson. Chem.*, 2000, **38**, 265.
16. K. E. Kovér, G. Batta, and K. Fehér, *J. Magn. Reson.*, 2006, **181**, 89.
17. T. Parella and J. Belloc, *J. Magn. Reson.*, 2001, **148**, 78.
18. M. Misiak and W. Kozminski, *Magn. Reson. Chem.*, 2008, **47**, 205.
19. T. Parella, J. Belloc, and F. Sánchez-Ferrando, *Magn. Reson. Chem.*, 2004, **42**, 852.
20. K. Kobzar and B. Luy, *J. Magn. Reson.*, 2007, **186**, 228.
21. V. V. Krishnamurthy, *J. Magn. Reson. A*, 1996, **121**, 33.
22. A. Meissner and O. W. Sørensen, *Magn. Reson. Chem.*, 2001, **39**, 49.
23. K. Furihata and H. Seto, *Tetrahedron Lett.*, 1999, **40**, 6271.
24. W. Willker and L. Leibfritz, *Magn. Reson. Chem.*, 1995, **33**, 632.
25. M. Findeisen and S. Berger, *Magn. Reson. Chem.*, 2003, **41**, 431.
26. G. Zhu, A. Renwick, and A. Bax, *J. Magn. Reson.*, 1994, **110**, 257.
27. K. Kobzar and B. Luy, *J. Magn. Reson.*, 2007, **186**, 131.
28. P. Nolis, M. Pérez, and T. Parella, *Magn. Reson. Chem.*, 2006, **44**, 1031.

